



Effect of germanium on the microstructure and the magnetic properties of Fe–B–Si amorphous alloys

D.C. Estévez*, I. Betancourt

Departamento de Materiales Metalicos y Ceramicos, Instituto de Investigaciones en Materiales, Universidad Nacional Autónoma de México, México D.F. 04510, Mexico

ARTICLE INFO

Article history:

Received 13 March 2012

Received in revised form 8 May 2012

Available online 4 June 2012

Keywords:

Soft magnetic properties;

Crystallization;

Ferromagnetic resonance

ABSTRACT

In this work, we present a systematic study on the crystallization kinetics and the magnetic properties of melt-spun $\text{Fe}_{80}\text{B}_{10}\text{Si}_{10-x}\text{Ge}_x$ ($x = 0.0 - 10.0$) amorphous alloys. The activation energy for crystallization, determined by differential scanning calorimetry, displayed a strong dependence on the Ge content, reflecting a deleterious effect on the alloys' thermal stability and their glass forming ability with increasing Ge concentration. On the other hand, the alloys exhibited excellent soft magnetic properties, i.e., high saturation magnetization values (around 1.60 T), alongside Curie temperatures of up to 600 K. Complementary, for increasing Ge substitution, the ferromagnetic resonance spectra showed a microstructural evolution comprising at least two different magnetic phases corresponding to a majority amorphous matrix and to Fe(Si, Ge) nanocrystallites for $x \geq 7.5$.

© 2012 Elsevier B.V. All rights reserved.

1. Introduction

Since the first amorphous alloy synthesized in the Au–Si system by rapid solidification [1], a large variety of metallic glasses have been developed during the subsequent four decades [2–9]. Among these materials, $\text{Fe}_{1-x}\text{B}_x$ -based glassy alloys (with $15 < x < 30$) have been used in a wide range of applications as magnetic materials due to their excellent combination of soft magnetic properties, including high values of saturation magnetization, magnetic permeability and Curie temperature, together with very low power losses [4]. In fact, their current use in power electronic devices render them as an important group of engineering amorphous alloys [10]. In order to tailor the magnetic performance of these materials, alloying with transition metals (Co, Ni, Zr, Nb, Hf) and metalloids or non-metals atoms (Si, Ge or C, P) have proved to be useful, since a strong dependence of main intrinsic magnetic properties (namely, saturation magnetization and Curie temperature) with such alloying elements have been described with profusion [11–18]. In spite of the numerous reports regarding the impact of chemical composition variations on the physical properties of FeB-based amorphous alloys [19–26] and some other reports including the influence of Ge in another alloy systems [27–32], comparatively not one study can be found in the literature concerning the influence of the progressive addition of Ge in FeBSi alloys on their microstructure and magnetic properties. In this work, a systematic replacement of Si by Ge in the alloy system $\text{Fe}_{80}\text{B}_{10}\text{Si}_{10-x}\text{Ge}_x$ ($x = 0.0 - 10.0$ at.%) has been studied in order to determine the influence of such additions on their microstructure and magnetic properties.

2. Experimental techniques

Master ingots of 5.0 g were prepared from high purity elements Fe (99.99 wt.%), B (99.96 wt.%), Ge (99.9 wt.%), Si (99.9 wt.%) in an Ar arc-melting unit and were remelted four times to ensure chemical homogeneity, with little changes (below 1 mass%) of their weight after remelting. Metallic ribbons (20–30 μm thickness and 1.8 mm width) for each composition of the alloy series $\text{Fe}_{80}\text{B}_{10}\text{Si}_{10-x}\text{Ge}_x$ ($x = 0.0, 2.5, 5.0, 7.5, 10.0$ at.%) were produced by means of melt spinning technique into a sealed chamber under He atmosphere at a roll speed of 40 m/s. The microstructure of the as-cast alloys was determined by means of X-ray diffraction analysis (XRD) in a Siemens D5000 diffractometer with $\text{Co-K}\alpha$ radiation and step size of 0.020° at 40 kV and 20 mA and by Transmission Electron Microscopy (TEM) in a Jeol 1200EX equipment operating at 120 kV. The crystallization kinetics was characterized by continuous heating in a differential scanning calorimeter (TA Instruments SDT Q600), by using variable heating rates between 5 and 25 K/min. As the reference plate the same empty aluminum capsule was used. On the other hand, room temperature magnetic measurements were carried out on as-quenched samples using Vibrating Sample Magnetometry (VSM) in a LDJ 9600 apparatus with a maximum applied field of 1360 kA/m, for which the uncertainty was estimated from the standard deviation after 10 repetitions. The equipment was calibrated using a high purity 2 mm nickel sphere of known mass and magnetic moment. Complementary, Curie temperature was determined using magnetic thermogravimetric analysis (MTGA) in a TA instruments 2950 thermobalance with a heating rate of 10 K/min, coupled with a permanent magnet. Ferromagnetic resonance (FMR) measurements were made by means of a Jeol JESRES3X spectrometer operating at 9.4 GHz (X-band) using horizontal-parallel orientation, i.e. the H_{dc} field is applied parallel the longitudinal ribbon axis and

* Corresponding author. Tel.: +52 44 5622 4642; fax: +52 44 5616 0754.
E-mail address: estevd@gmail.com (D.C. Estévez).

perpendicular to the H_{ac} field. Random errors are minimized due to the high precision ($\pm 1\%$) for both, MTGA and VSM techniques (according to the instruments manual). On the other hand, a careful calibration procedure for all equipments was performed with the proper standards in each case in order to preclude systematic errors.

3. Results

3.1. Microstructure

XRD diffractograms for all the alloy ribbons are shown in Fig. 1. Initial compositions present a single broad peak indicative of a fully glassy structure, as confirmed by TEM observations, which exhibits a single diffuse halo (see inset in Fig. 1 corresponding to $x=0.0$). By contrast, for samples with $x=7.5$ and $x=10.0$, some additional peaks are observed at $2\theta=52.7^\circ$ ($x=7.5$) and at $2\theta=52.48^\circ$ and 77.18° ($x=10.0$) which were associated to the (110) and (220), (620) planes of the cubic $Fe_3(Si, Ge)$ and the Fe_3Ge phases, respectively (according to the ICDD files 065-0994 and 03-065-9102). These diffraction peaks are indicative of a progressive crystallization process upon Ge substitution. For $x=10.0$, an increased crystallized volume fraction is supported by the TEM micrographs displayed in Fig. 2, for which a composite structure comprising an amorphous phase together with small precipitates lower than 20 nm (Fig. 2a) is observed. The corresponding diffraction pattern (Fig. 2b) includes some few spots immersed into the diffuse haloes, related to additional crystallization of the residual amorphous phase present in the samples after the initial crystallization. They correspond to the (111), (200), (220), (222) and (400) diffraction planes of the Fe_3Ge phase. These crystalline inclusions are proof of the growth of the Fe_3Ge crystalline phase from the amorphous matrix. The well-defined splitting on the diffraction rings indicates that the crystallites possess long-range order.

3.2. Crystallization kinetics and glass forming ability

Fig. 3 shows DSC curves for the $Fe_{80}B_{10}Si_{10-x}Ge_x$ alloy series, measured at a heating rate of 25 K/s. For Ge concentrations $x < 10$, all plots exhibit a two-step crystallization process, with two widely separated exothermic peaks. In each one there is an overlapped exothermic peak, it means that the first stage of crystallization occurred simultaneously in the samples with a primary crystallization peak T_{x1} between 716 K and 760 K, and a secondary crystallization peak T_{x2}

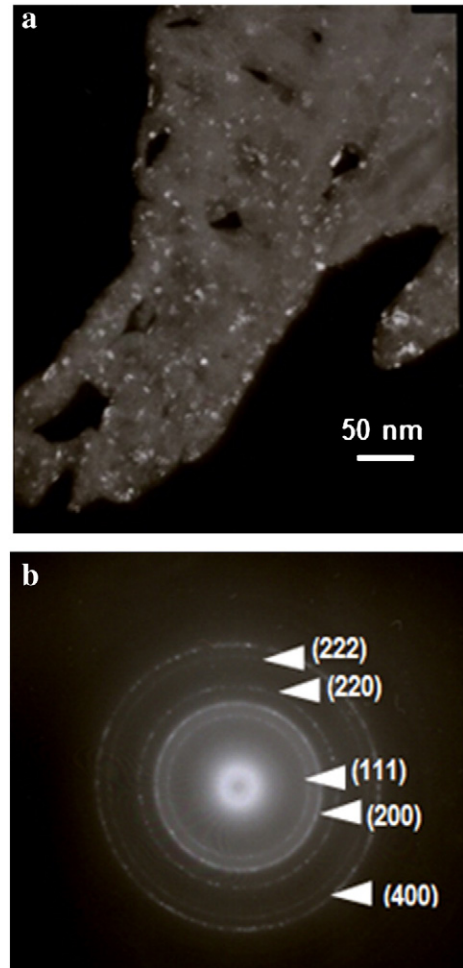


Fig. 2. TEM micrographs for the $Fe_{80}B_{10}Ge_{10}$ alloy: a) Dark field image exhibiting the nanocrystalline phase Fe_3Ge embedded in an amorphous matrix; b) the corresponding diffraction pattern (planes are indexed with the Fe_3Ge phase).

above 800 K. The $Fe_{80}B_{10}Ge_{10}$ alloy sample exhibits no crystallization event, which is consistent with XRD and TEM results. For increasing Ge content, T_{x1} decreases, reflecting a reducing thermal stability upon

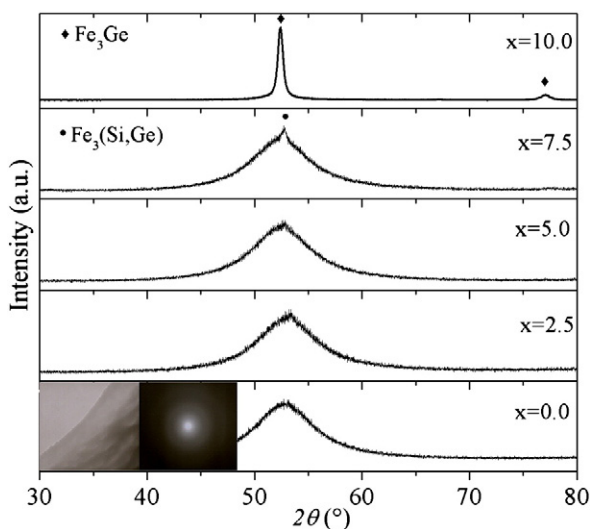


Fig. 1. XRD diffractograms and TEM micrographs for the $Fe_{80}B_{10}Si_{10-x}Ge_x$ alloy series. Inset: TEM micrograph and the corresponding selected area diffraction pattern for the $Fe_{80}B_{10}Si_{10}$ alloy sample.

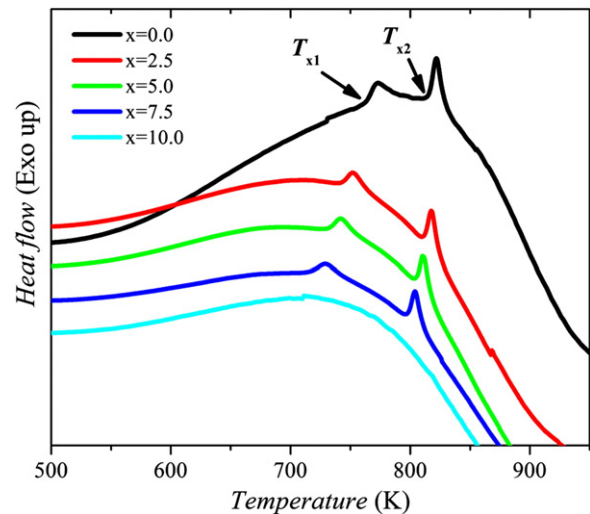


Fig. 3. DSC curves for the $Fe_{80}B_{10}Si_{10-x}Ge_x$ alloy series at a heating rate of 25 K/s. The two-step crystallization process of the amorphous phase is clearly manifested as exothermic reactions, for which the primary and secondary temperatures T_{x1} and T_{x2} indicate the onset of each event.

Download English Version:

<https://daneshyari.com/en/article/1481543>

Download Persian Version:

<https://daneshyari.com/article/1481543>

[Daneshyari.com](https://daneshyari.com)